



HAL
open science

Matrix-driven environmental fate and effects of silver nanowires during printed paper electronics end of life

Andrea Carboni, Danielle Slomberg, Amazigh Ouaksel, Lenka Brousset, Andrea Campos, Bernard Angeletti, Bahareh Zareeipolgardani, Gael Depres, Alain Thiéry, Jerome Rose, et al.

► To cite this version:

Andrea Carboni, Danielle Slomberg, Amazigh Ouaksel, Lenka Brousset, Andrea Campos, et al.. Matrix-driven environmental fate and effects of silver nanowires during printed paper electronics end of life. *Environmental science.Nano*, 2023, 10 (11), pp.3039-3050. 10.1039/D3EN00263B . hal-04291887

HAL Id: hal-04291887

<https://cnrs.hal.science/hal-04291887>

Submitted on 17 Nov 2023

HAL is a multi-disciplinary open access archive for the deposit and dissemination of scientific research documents, whether they are published or not. The documents may come from teaching and research institutions in France or abroad, or from public or private research centers.

L'archive ouverte pluridisciplinaire **HAL**, est destinée au dépôt et à la diffusion de documents scientifiques de niveau recherche, publiés ou non, émanant des établissements d'enseignement et de recherche français ou étrangers, des laboratoires publics ou privés.

1 Matrix driven environmental fate and effects of silver nanowires during printed paper electronics end
2 of life

3

4 Andrea Carboni,^{1,2,*} Danielle L. Slomberg¹, Amazigh Ouaksel¹, Lenka Brousset³, Andrea Campos⁴,
5 Bernard Angeletti¹, Bahareh Zareeipolgardani⁵, Gael Depres⁵, Alain Thiéry³, Jerome Rose^{1,7}, Laurent
6 Charlet⁵ and Melanie Auffan^{1,7}

7

8

9 ¹ CNRS, Aix-Marseille Univ., IRD, INRAE, CEREGE, 13545 Aix-en-Provence, France

10 ² Dipartimento di Chimica "Giacomo Ciamician", Alma Mater Studiorum-Università di Bologna, Via
11 Francesco Selmi 2, 40126 Bologna, Italy

12 ³ CNRS, IRD, IMBE, Aix-Marseille Univ, Avignon Univ., Marseille, France

13 ⁴ CNRS, Aix Marseille Université, Centrale Marseille, FSCM (FR1739), CP2M, 13397 Marseille, France

14 ⁵ Université Grenoble Alpes, Université Savoie Mont Blanc, CNRS, IRD, IFSTTAR, ISTerre, Grenoble
15 38400, France

16 ⁶ Fedrigoni, 10 Rue Jean Arnaud, 38500 Voiron, France

17 ⁷ Civil and Environmental Engineering Department, Duke University, Durham, North Carolina 27707,
18 United States

19

20

21 Corresponding author

22 Andrea Carboni, Dipartimento di Chimica "Giacomo Ciamician", Alma Mater Studiorum-Università di
23 Bologna, Via Francesco Selmi 2, 40126 Bologna, Italy

24 andrea.carboni@unibo.it

25 orcid.org/ 0000-0002-5156-4645

26

27

28

29

30

31

32

33

34

35 *Abstract*

36

37 *The release of engineered nanomaterials (ENMs) during manufacturing, use and disposal of nano-*
38 *enabled products (NEPs) is a potential route of environmental nano-pollution. To date, there is limited*
39 *knowledge on the ecological impact of ENMs incorporated in NEP matrices and how they compare to*

40 *pristine nanoparticles. Here, we examined the fate and effect of silver nanowires (AgNWs) embedded in*
41 *a cellulose matrix for the production of printed paper electronics (PPE) (nano)technologies. The fate and*
42 *impact of fragmented AgNWs-PPE was monitored for 21 days in freshwater mesocosms mimicking a*
43 *pond ecosystem. The Ag release and AgNWs-PPE behavior in water was further characterized in abiotic*
44 *batch incubations. Qualitative and quantitative analysis were carried out to estimate the Ag partitioning*
45 *between the environmental compartments and the aging of AgNWs-PPE as well as bioaccumulation*
46 *and behavior responses in biota.*

47 *In contaminated pond mesocosms, the NEP cellulose/ polyvinylidene chloride matrix resulted in a rapid*
48 *settling of the Ag onto the sediments and prevented Ag release into the water column. The highest*
49 *aqueous concentration measured corresponded to less than 0.5% of the total Ag introduced. The*
50 *AgNWs-PPE fragments accumulated at the water sediment interface, where they were rapidly*
51 *(bio)degraded and became bioavailable for benthic organisms. Aquatic snails accumulated a significant*
52 *fraction of the Ag ($1.4 \pm 0.5\%$) and displayed enhanced burrowing behavior in comparison to controls.*

53 *In batch experiments, alteration of the ENMs morphology was evident at the NEPs surface. Here, the*
54 *colocalization of Ag and S clusters, suggest an aging via sulfidation similar to other pristine Ag-ENMs.*
55 *However, the cellulose matrix prevented weathering of the AgNWs within the NEP, which presented a*
56 *near pristine state even after 21 days incubation.*

57 *Overall, these results indicate that the fate and impact of Ag embedded in the AgNWs-PPE was driven*
58 *by the cellulose matrix. In particular, given the specific properties and behavior of paper-based*
59 *(nano)products, these may constitute a unique category when evaluating NEPs environmental impact.*
60 *The data gathered in this study can help in defining the environmental fate of such materials and*
61 *provide useful information to address future studies focused on ENM environmental fate and risk*
62 *assessment in a life-cycle perspective.*

63

64

65

66

67 **Keywords**

68 Nano-enabled products, printed paper electronics, mesocosms, silver nanomaterials, aquatic
69 ecosystem

70

71

72

73

74 **1. Introduction**

75

76 Nanotechnologies are expected to impact our future with the development of safer and sustainable
77 solutions in the context of the environmental and energetic transition(1). In this framework, green
78 (nano)technologies such as printed paper electronics (PPE) devices are an emerging and potentially

79 game-changing technology, due to ease of recycling, economics of manufacture and applicability to
80 flexible electronics(2). However, the environmental safety and sustainability aspects of nano-enabled
81 products (NEPs) are being investigated at a relatively slow pace compared to their development and
82 commercialization(3). Recently, silver nanowires (AgNWs) have gathered attention in PPE due to
83 their excellent optoelectronic properties, ease of processing, and large-scale fabrication capability(4).
84 An expected promising application of AgNWs-based PPE is the production of sensors and electric
85 device displays of high transparency, flexibility, and stretchability(5).
86 Although AgNWs-based PPE can represent a robust, more sustainable and eco-friendly alternative to
87 conventional ones, knowledge on their environmental risk is largely unknown(2)(6). Furthermore,
88 the existing data sets generated from exposure and hazard studies with pristine Ag-based ENMs
89 could not be representative of Ag-based NEPs behavior, fate and hazard and are inadequate to
90 support meaningful regulation and assessment tasks(7). Previous studies on Ag-NEPs showed that
91 their environmental fate and impact strongly depends on manufacturing processes (i.e. with Ag
92 ENMs applied as surface coating or embedded in the product matrix), the initial ENM load and the Ag
93 speciation(8)(9)(10)(11). The NEPs matrix is also an important factor driving ENMs fate, and was
94 proposed as a main criteria when grouping NEPs eco-toxicity during the use phase(12). Pourzahedi et
95 al.,(13) performed a life cycle assessment of 15 Ag-NEP (textiles and medical fabrics) and highlighted
96 the role of the matrix, with solid polymeric matrices releasing more silver during washing compared
97 to fibrous materials.
98 A recent study investigated the fate of AgNWs printed on PPE (AgNWs-PPE) during a pilot-scale
99 recycling process(14), showing that the released effluents were free from Ag, which was retained in
100 the pulp conserved for recycling. The main aim of the present study was to mimic a chronic
101 contamination of an aquatic ecosystems by AgNWs-PPE to assess, at environmentally relevant
102 conditions, the fate and effects upon release in the environment.
103 Given the expected long PPE lifetime, compared to the experiment duration, a pre-aging protocol
104 was applied. In particular, the AgNWs-PPE samples were fragmented in order to obtain a fragmented
105 product (FP), resulting in an increased surface area at the NEP/ecosystem interface(15). Mesocosms
106 allow for simulating realistic ecological conditions, and experiments can be designed to study the
107 aging of ENMs while characterizing the associated exposure and hazard(16)(17)(18). In the last years,
108 such experimental systems have been extensively applied for the study of ENM fate
109 e.g.(19)(20)(21)(22) , but to a lesser extent to NEP(23)(24). Using freshwater mesocosms, we first
110 characterized the partitioning of Ag between the environmental compartments. The results obtained
111 with AgNWs-PPE were compared to pristine AgNWs in order to identify the potential role of the
112 matrix in determining the Ag partitioning. Complementary mechanistic abiotic batch experiments
113 were used to further characterize the fate of the NEP and incorporated ENMs. Eventually, we also
114 investigated the bioaccumulation into benthic grazers and assessed behavioral markers, which can
115 be sensitive tools at concentrations far below the lethal effect(25).
116 This study provides realistic environmental exposure data, which are needed to inform decision-
117 making to mitigate or manage the risks associated to ENMs and NEPs.

118

119

120 2. Materials and methods

121

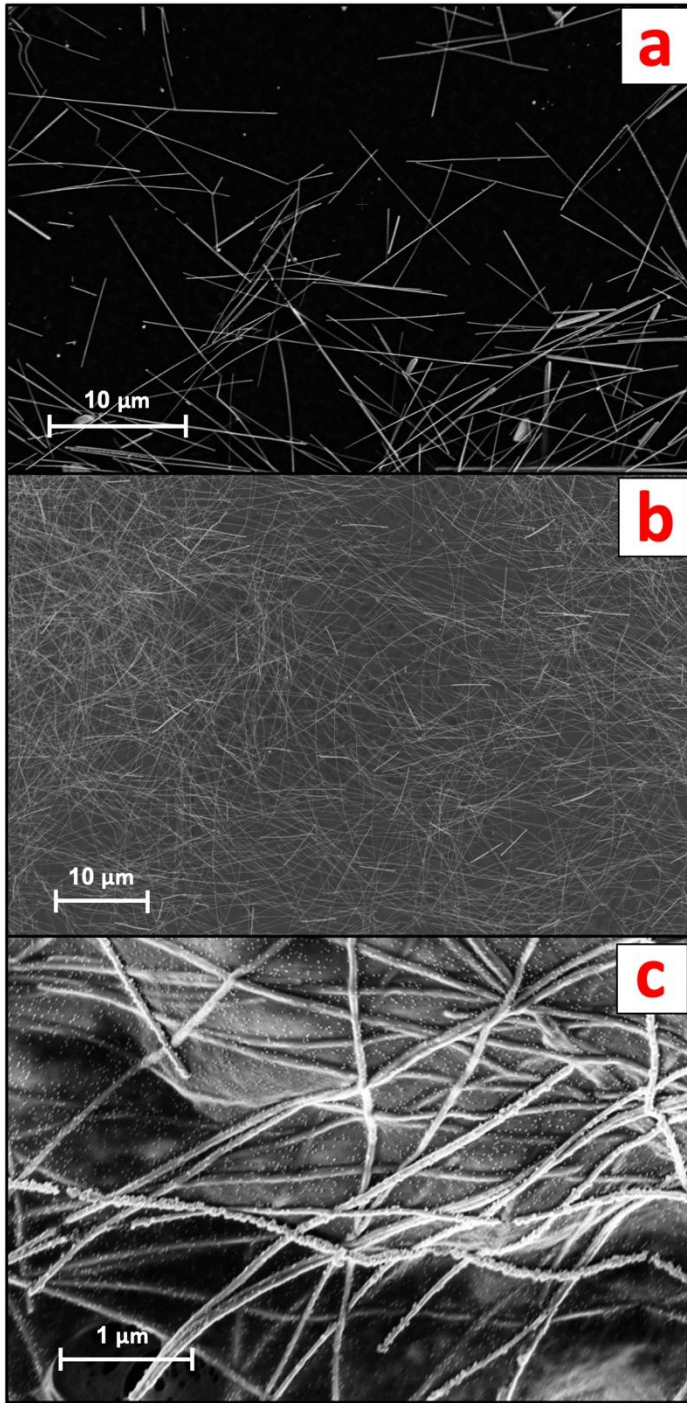
122 2.1. PPE and AgNWs

123

124 The AgNWs suspensions were obtained by diluting a commercial standard (nominal 120 μm AgNWs
125 length, 20 $\text{g}[\text{Ag}]\cdot\text{L}^{-1}$ in water; ACS material, CA, US) in ultrapure water (UPW; Milli-Q®, Merck,
126 Germany). The AgNWs, characterized by scanning electron microscopy (SEM) coupled to Energy
127 Dispersive X-Ray Spectroscopy (EDX), displayed an average width of 94.3 ± 8.5 nm and an average
128 length of 13.1 ± 4.3 μm ($n=40$) (Fig. 1a).

129 The AgNWs-PPE samples were received from Arjowiggins now Fedicroni Co. (Voiron, France), as
130 210mm x 297mm sheets consisting of three distinct layers, namely made of cellulose, an organic
131 coating and conductive ink, respectively. Briefly, a 60 μm thick mixed-cellulose nanofibrils (CNF)
132 matrix was coated, on one side, with a layer of polyvinylidene chloride (PVDC, 5 μm thickness). A
133 conductive ink layer (200-300 nm in thickness) incorporating nano-cellulose fibers and the AgNWs
134 was applied on top of the organic coating, resulting in a sheet resistance of approximately 30 Ω/sq
135 across the samples. The concentration of Ag in the final AgNWs-PPE samples was 1.38 ± 0.07 $\text{mg}\cdot\text{g}^{-1}$.

136 For both the mesocosm and abiotic batch experiments, the original AgNWs-PPE sheet samples were
137 fragmented, in order to mimic the potential physical-chemical form at which the NEPs are released
138 in the environment during the use phase. The protocol for fragmentation was optimized from
139 procedures reported in the literature(12)(15)(24). First, the PPE samples were cut with a ceramic
140 blade to approximately 2 x 2 mm fragments and transferred into 2 ml plastic vials (Eppendorf,
141 Hamburg, Germany). Then, two zirconium marbles were added in each of the vials, which were
142 loaded into a Teflon sample holder and soaked into liquid nitrogen. The frozen samples underwent
143 two 30 sec cycles of ball-milling at 30 Hz (Mixer Mill MM400, Retsch). Liquid nitrogen was poured
144 between the two fragmentation cycles to prevent unfreezing. Finally, a sieving at 0.5 mm was
145 performed in order to remove the largest PPE fragments. The AgNWs-PPE fragments size, assessed
146 with optical microscopy was 107.2 ± 72.2 μm on average ($n=180$). As shown in Fig. 1b, in AgNWs-PPE
147 fragments the ENMs were homogeneously distributed onto the NEPs, and displayed average
148 diameter of 81.0 ± 11.1 nm and average length of 15.6 ± 3.5 μm ($n=40$). At the AgNWs-PPE surface,
149 the AgNWs formed entanglements, displaying protruding nano-structures as well as portions
150 merged within the cellulose matrix (Fig. 1c).



151
152
153
154
155
156
157
158

Figure 1. Scanning electron microscopy analysis of the pristine ENM and NEP in this study. a) The pristine AgNWs standard (7kV, VP BSE detector). b) The homogeneous surface distribution of AgNWs onto the AgNWs-PPE cellulose matrix (7kV, VP BSE detector). c) A close-up of the AgNWs at the AgNWs-PPE surface (0.5 kV, In Lens SE detector).

159

160 2.2. Mesocosm set-up and operation

161

162 Nine indoor aquatic mesocosms were set up to mimic a natural pond ecosystem in the preserved
163 Natura 2000 reserve network, southern France (43.34361 N, 6.259663 E, altitude 107 m a.s.l.,
164 Mediterranean climate). Natural sediments, natural water and organisms were collected at the site
165 within 3 days before setting up the mesocosms. Natural sediments were consecutively sieved at 2
166 mm and 250 μm in order to obtain a homogeneous inoculum containing primary producers (e.g.,
167 algae, bacteria). Natural water samples were first sieved at 250 μm and then filtered at 0.2 μm in
168 order to collect suspended matter and biota onto the glass fiber filters. The filters were then placed
169 into 1.5 L Volvic[®] water under constant agitation for 48 hrs.

170 Each mesocosm consisted of a glass tank (750 × 200 × 600 mm) consecutively filled with a layer of
171 artificial sediment (79% SiO_2 , 20% kaolinite, and 1% CaCO_3) covered with 300 g of water-saturated
172 natural sediment inoculum (48% water content) and 46 L of Volvic[®] water, with pH and conductivity
173 values similar to those of the natural pond water. After one week, 0.1 L of water inoculum was added
174 to each aquarium. The mesocosms operated on a 14 h day, 10 h night lighting period. Additional
175 details about mesocosm set-up and monitoring can be found in Auffan et al. (2014)(20). The set-up
176 was followed by an equilibration period of two weeks, in order to allow the settling of suspended
177 matter, stabilization of the physico-chemical parameters (pH, oxidation–reduction potential [ORP],
178 dissolved O_2) and the development of the primary producers(26). After the equilibration period,
179 organisms were introduced at a density matching the one observed in the natural biotope. In each
180 mesocosm, 70 mollusks (*A. leucostoma* (Millet 1813), benthic grazers) and 90 micro-crustaceans
181 (*Daphnia* sp., (Muller 1785), planktonic filter feeders) were added. Three days after the addition of the
182 organisms, the mesocosms were randomly assigned to either contaminated or non-contaminated
183 (control) treatments. Contamination was achieved by chronic (press) addition of either fragmented
184 AgNWs-PPE or pristine AgNWs three times per week (9 injections in total) during 21 days. Spiking
185 suspensions were prepared in UPW immediately before addition, vigorously stirred and
186 homogeneously distributed at the water surface. In AgNWs-PPE treatments, each contamination
187 consisted of 175 mg of AgNWs-PPE fragments, corresponding to single Ag doses of 241 μg and a final
188 concentration of 46.7 $\mu\text{g}[\text{Ag}].\text{L}^{-1}$ in the mesocosms. Such a dose was selected as a compromise
189 between the low levels expected in the real ecosystems and the possibility to analyze and
190 characterize the AgNWs-PPE in complex environmental matrices. For AgNWs treatments, single Ag
191 doses of 2.42 mg led to concentration of 470 $\mu\text{g}[\text{Ag}].\text{L}^{-1}$ at the end of the experiment. Such a dose
192 corresponded to a ENMs-surface to mesocosm water ratio of $1.9 \times 10^{-3} \text{ m}^2.\text{L}^{-1}$ (at day 21), and was
193 chosen to match the values recently used for other Ag-ENMs in mesocosms(27).

194

195 2.3. Mesocosm sampling and analysis

196

197 Several abiotic and biotic parameters were monitored to inform about the exposure and effects of
198 contamination on the aquatic ecosystem. These included the continuous measurements of water
199 physical-chemical properties (pH, oxidation-reduction potential (ORP), electrical conductivity,
200 temperature, dissolved oxygen) as well as punctual measurements of biotic parameters (Ag
201 concentration in water column, sediment and organisms, bacterial counting, total organic carbon
202 content (TOC), number of suspended particles and chlorophyll concentration(20)(26)).

203 A first aim of the present study was to quantify the distribution of Ag in the mesocosm following
204 AgNWs or AgNWs-PPE contamination. For this purpose, superficial sediments, the water column
205 and the aquatic snails *A. leucostoma* were sampled prior to contamination and then after 7, 14 and 21
206 days. For water column samples, 10 mL were collected at approximately 10 cm below the water
207 surface, transferred into 15 mL plastic tubes and acidified with 2% ultrapure HNO₃ (Normatom[®];
208 SCPScience, Quebec, Canada). Additional 5 mL water samples underwent ultrafiltration at 3 KDa
209 (Amicon Millipore; Merck KgaA, Darmstadt, Germany) prior to analysis, for the assessment of
210 dissolved Ag concentrations.

211 Surficial sediment and *A. leucostoma* samples were dried for 3 days at 65 °C, manually ground in an
212 agate mortar, and then transferred into 15 mL Teflon tubes. 50 mg of each sample was processed as
213 follows. For sediments, 1 mL HCl (34%) (Normatom[®]), 2 mL HNO₃ (67%) and 0.5 mL HF (47–51%,
214 PlasmaPure[®]) were added. For *A. leucostoma*, an additional 0.5 mL of H₂O₂ (30–32%, PlasmaPure[®])
215 was added. Then, acid digestion was performed at 180 °C in a Milestone UltraWAVE microwave
216 digestion system for 1 h. The metal analysis was performed with an inductively coupled plasma mass
217 spectrometer (ICP-MS, Nexlon 300X, Perkin Elmer[®]).

218

219 2.4 Abiotic batch aging experiments

220 In parallel to the mesocosm experiment, an abiotic batch experiment was carried out for 21d in 250
221 mL glass beakers, filled with 200 ml Volvic[®] water to gather mechanistic information on the aging of
222 the AgNWs-PPE fragments in abiotic conditions close to those in the mesocosm (e.g. water
223 composition, temperature, day/night cycle). Dosing was carried out with a single addition (pulse
224 dosing) of fragmented AgNWs-PPE at day 0 to match the final dose used in AgNWs-PPE mesocosms
225 (50 µg[Ag].L⁻¹).

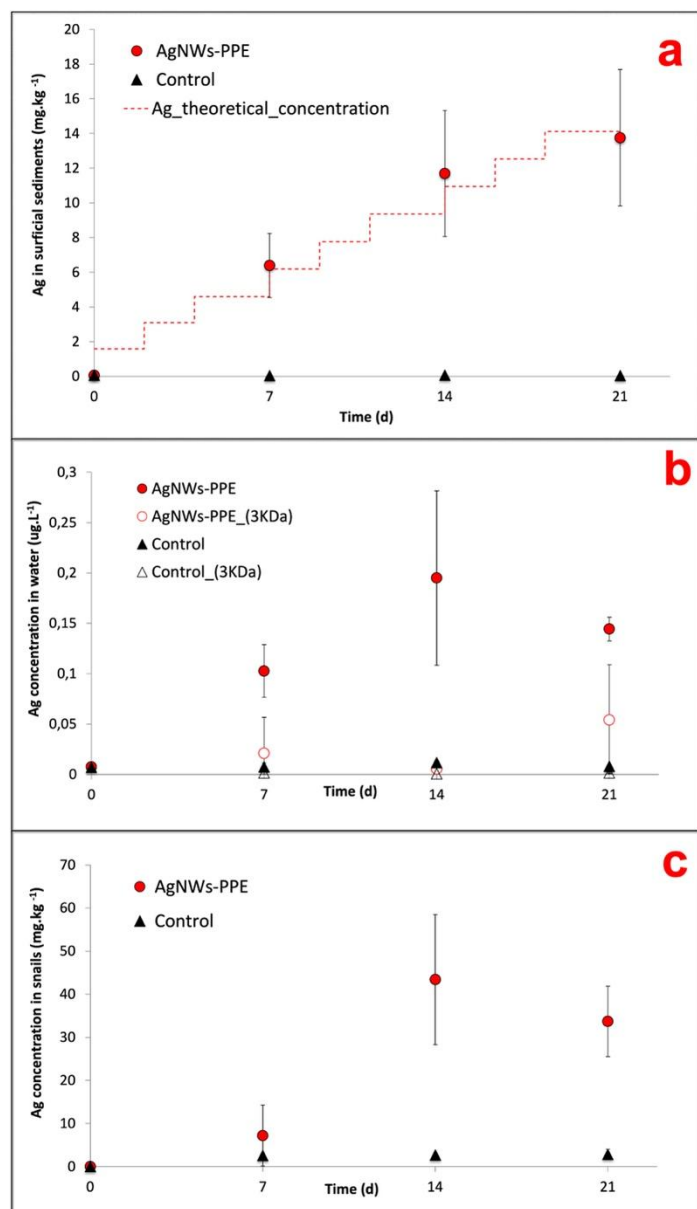
226 In the abiotic batch experiment the water was sampled similar to the mesocosms for total and
227 dissolved (<3KDa) Ag concentrations. In addition, at the end of the experiment the AgNWs-PPE were
228 recovered from the beakers, rinsed with UPW and transferred onto glass petri dishes. The excess
229 water was removed with a pipette and the samples were let to dry at room temperature in the dark.
230 The dried samples were stored at 4 °C in the dark for elemental and SEM analysis.

231 SEM analysis was performed with a Zeiss GeminiSEM 500 ultra-high resolution Field Emission
232 Electron Microscope. For imaging, this system was equipped with a column-mounted detector for
233 high efficiency surface secondary electron detection (In Lens SE) as well as variable pressure
234 secondary electron (VPSE) and variable pressure backscattered electron (VP BSE) detectors to
235 observe non-conductive samples. The surface analysis of a region of interest was acquired first at low

236 voltage (0.5 kV, In Lens SE detector) to increase topographic contrast and reduce specimen charging,
237 and then at higher energy (7 kV, VP BSE detector), to analyze a deeper fraction of the samples and
238 for Energy Dispersive X-ray Spectroscopy (EDX) acquisition. The electron acceleration tension was
239 set at 7 kV in order to achieve sufficient X-ray emission to detect Ag L lines at 3 keV, whereas analysis
240 at higher energies was not possible due to irreversible damage of the PPE matrix. For the chemical
241 imaging, EDX was performed using an EDAX Octane Silicon drift detector (129 eV energy resolution
242 for Manganese). During SEM-EDX mapping, the dwell time for each point was set to 50 μ s per pixel
243 and frames were accumulated with drift correction. Reference images taken at the beginning of the
244 acquisition were periodically checked to monitor the potential alteration of the samples during
245 measurements.
246

247 3. Results and discussion

248
249 3.1. NEP matrix-driven accumulation of Ag on the surficial sediments



250
251

252 Figure 2. (a) Total concentration of Ag in the superficial sediments, (b) total and dissolved (<3KDa) Ag
253 concentrations in the water column, and (c) total concentration of Ag in *A. leucostoma* in mesocosms
254 contaminated with AgNW-PPE versus controls. Dotted-line in (A) represents the concentration
255 expected if all the Ag added to the mesocosms settled at the surface of the sediments. Error bars
256 indicate the standard deviation between mesocosms in the same treatment (n=3).

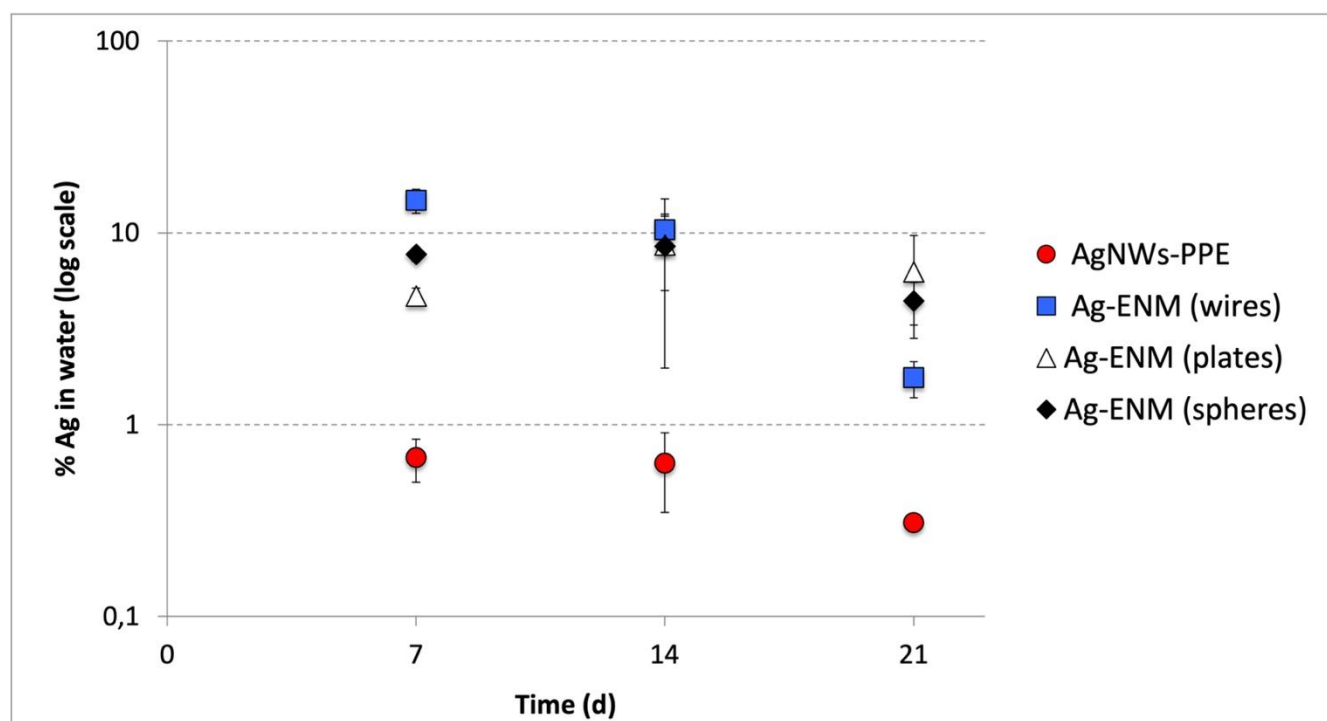
257
258

259 In AgNWs-PPE contaminated mesocosms, the Ag concentration in the sediments increased with the
260 time to values significantly higher than those of the controls (Fig. 2a). In detail, following chronic
261 exposure of AgNWs-PPE fragments, the Ag in the sediments was $6.4 \pm 1.8 \text{ mg.kg}^{-1}$ after 7 days and
262 reached $13.8 \pm 3.9 \text{ mg.kg}^{-1}$ at the end of the experiment. These results indicate that the benthic
263 compartment was the main sink for Ag in the simulated pond ecosystem, accumulating up to
264 $97 \pm 28\%$ of the total Ag injected at 21d. The Ag partitioning toward the sediments was accompanied
265 by its minor presence in the water column (Fig. 2b) with a total aqueous concentration of Ag reaching
266 $0.10 \pm 0.03 \text{ } \mu\text{g.L}^{-1}$ after 7d. This concentration in the water column remained stable until the end of
267 the experiment with $0.19 \pm 0.08 \text{ } \mu\text{g.L}^{-1}$ at 14d and $0.14 \pm 0.01 \text{ } \mu\text{g.L}^{-1}$ at 21d, corresponding to
268 approximately 0.5% of the Ag initially introduced. This is in agreement with the macroscopic
269 observation of the fast settling down of the AgNWs-PPE fragments right after the injection in the
270 mesocosm surface water. Furthermore, no significant Ag was measured in water after ultrafiltration,
271 indicating either the lack of Ag dissolution or the rapid removal of Ag dissolved species from the
272 water column via reprecipitation or complexation, which was already observed in previous
273 studies(26)(28). It must be noted that the Ag species released from the AgNWs-PPE may also be
274 retained by the ultrafiltration membrane applied, because associated to NEP product matrix (e.g.
275 Ag-cellulose complexes) or due to absorption onto the membrane.

276 In freshwater mesocosms, important ENM removal from the water column is well known and has
277 been reported for a variety of ecosystem settings and nanomaterials tested. Previous studies,
278 focused on pristine Ag-ENMs with a similar contamination scenario (i.e. chronic dosing at similar Ag
279 total doses), reported comparable accumulation in sediment for a range of Ag-ENMs differing in
280 coatings and morphology. For instance, in pond indoor mesocosms contaminated with Ag-ENM
281 plates, the surficial sediments accumulated $85 \pm 19\%$ of the Ag after 28 d of chronic exposure(21)(27).
282 In these cases, compartmentalization into sediments was attributed to ENMs homo-aggregation
283 phenomena as well as hetero-aggregation with natural organic matter and suspended solids(19)(26).
284 In this study, AgNWs-PPE fragments were observed to settle rapidly after spiking into the mesocosm
285 surface water, suggesting that the sediment accumulation was likely driven by the cellulose matrix.

286 Nonetheless, the Ag released in water from the AgNWs-PPE was unexpectedly low for such a surface
287 coated NEP. Indeed, the silver metal and ENM species release from NEPs is known to rely on the
288 product matrix and manufacturing(8)(11). In general, high release rates can be expected for ENMs
289 present at the surface, compared to those incorporated into the NEP bulk(3)(12). For instance, in
290 freshwater aquatic mesocosm studies the Ag released from Ag-NEP surface coated textiles displayed
291 higher aqueous concentration and persistence compared to pristine Ag-ENMs(23). On the contrary,
292 ENMs included into materials such as acrylic paint displayed diminished release in water(24). Here,
293 although the AgNWs were present at the surface of the PPE, the Ag partitioning resembled that
294 observed for ENMs incorporated into NEPs such as paint nanocomposite(24). Such behavior could be
295 due to the ecosystem physical-chemical properties but also to the low hydrolysis of the cellulose
296 matrix preventing the short-term Ag release in water as well as the intrinsic physical-chemical

297 properties of AgNWs (e.g. size, morphology and surface chemistry) that can drive their
298 environmental fate.
299



300
301 Figure 3. Comparison between the Ag partitioning in the aqueous phase (% of total Ag introduced) of
302 AgNWs-PPE (red) and pristine AgNWs (wires, blue), Ag nano-plates (plates, white) and Ag nano-
303 spheres (spheres, black). *Ag nano-plates and Ag nano-spheres data with permission from Auffan et al.*
304 *(2020)(27)*.

305
306 To elucidate the role of the PPE matrix in determining the Ag behavior, the Ag partitioning following
307 AgNWs-PPE treatment was compared to that of pristine AgNWs (this study) as well as other pristine
308 Ag nano-plates and nano-spheres recently investigated in freshwater mesocosms by our team(27).
309 For this purpose, the AgNWs were dosed into mesocosms at similar surface area-based
310 concentrations as the ones used for Ag nano-plates and nano-spheres (Auffan et al., 2020)(27). As
311 shown in Fig. 3, in mesocosms contaminated with pristine AgNWs, the percentage of injected Ag
312 found in the water column was in the same range of magnitude than those previously observed for
313 Ag nano-sphere and nano-plates. The average Ag aqueous fraction of all the pristine Ag-ENMs was
314 $9 \pm 1\%$ at 14d and $4 \pm 2\%$ on average at 21d. Hence, for a given surface area-based concentration the
315 Ag release and water persistence are similar between Ag-ENMs of different shape and size.
316 In mesocosms contaminated with AgNWs-PPE, the water Ag fraction was lower than that of pristine
317 Ag-ENMs at all the time intervals ($0.5 \pm 0.2\%$ in average). In particular, when compared to pristine
318 AgNWs, the AgNWs-PPE aqueous Ag was 20-fold lower at 7d and 6-fold lower at 21d. These results

319 support the hypothesis that the Ag partitioning observed in AgNWs-PPE treatments was driven by
320 the NEP matrix and not by the specific properties of the AgNWs contained therein.

321

322

323

324 3.2. Mechanisms of AgNMs-PPE aging in freshwater environments

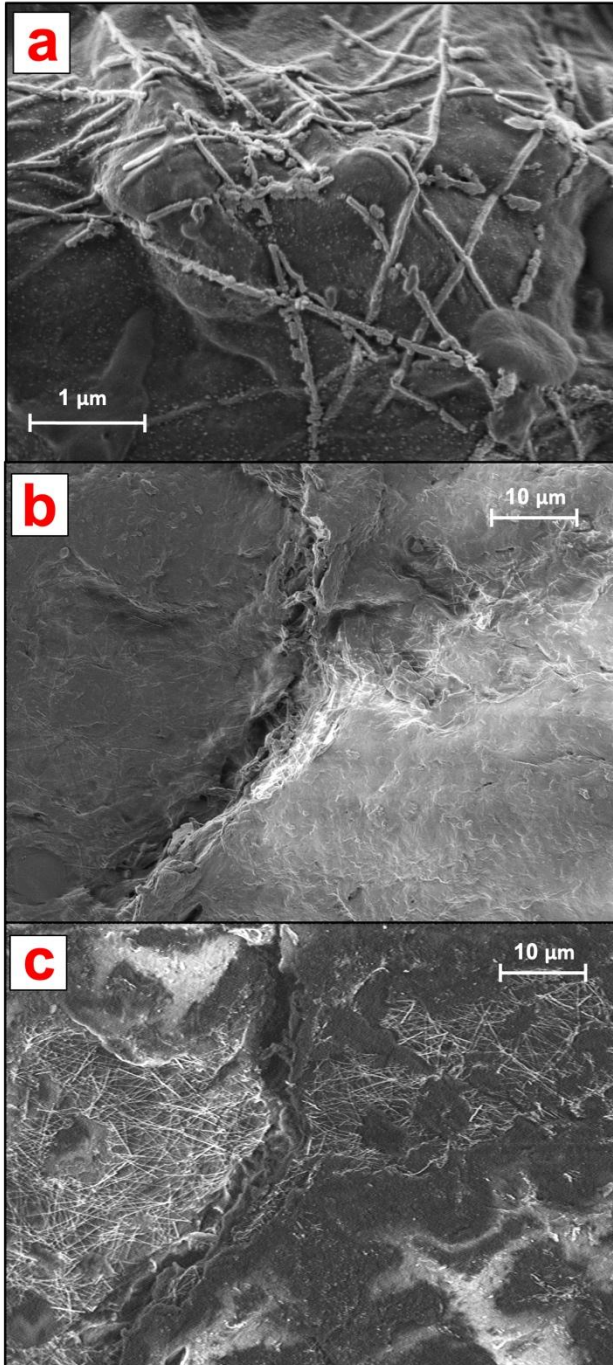
325

326 When assessing the AgNWs-PPE and Ag fate in freshwater mesocosms, a major limitation was due
327 to the impossibility to recover the aged NEP fragments. In particular, the AgNWs-PPE accumulated
328 onto the sediment formed flocs, which mixed with and were degraded by mesocosm's abiotic
329 (mineral sediment matrix) and biotic (biofilm and benthic organisms) components. In order to
330 monitor the AgNWs-PPE transformation and obtain quantitative and qualitative information, we
331 carried out batch experiments in simplified abiotic conditions. Here, the fragmented AgNWs-PPE
332 was incubated in static conditions, similar to the mesocosm experiment with regard to all the abiotic
333 parameters such as water chemistry, irradiation and temperature.

334 In the batch experiment, the concentrations of Ag in the water increased during the first week and
335 remained stable until the end of the incubation (Supplementary Information, S1). At day 21 the water
336 [Ag] reached $0.93 \pm 0.47 \mu\text{g}\cdot\text{L}^{-1}$, which was 5-fold higher than the maximum water concentration
337 measured in the mesocosms. This could be related to the lack of natural suspended matter (e.g.
338 organic matter, colloids) and biota (micro- and macro-organisms), in the batch system, which likely
339 play a role in the removal of dissolved or particulate Ag from the mesocosm water column. At the
340 end of the abiotic incubation up to $90.6 \pm 3.1 \%$ of the total Ag was found in the aged NEP fragments
341 recovered and the [Ag] measured after ultrafiltration was negligible indicating no free Ag ions in
342 solution.

343 Overall, these results suggest that the Ag remained associated with the NEP matrix, and highlight a
344 matrix driven Ag fate, suggesting that the contamination of aquatic ecosystems to such
345 cellulose/PVDC-based NEPs predominantly involves the exposure to Ag-PPE complexes rather than
346 free-ENMs and metal species.

347



348
349
350
351
352
353
354
355
356

Figure 4. SEM analysis at the surface of aged AgNWs-PPE samples (21d abiotic batch incubation). a) High magnification image taken at 0.5 keV showing the alteration and fragmentation of the AgNWs at the NEP aged surface. b) Image of larger AgNWs-PPE fragments area with low voltage acquisition (0.5 kV, In Lens SE detector) showing a limited presence of ENMs at the surface. c) The image of the same area acquired at higher voltage (7 kV, VP BSE detector) revealed a higher presence of AgNWs in the cellulose matrix bulk.

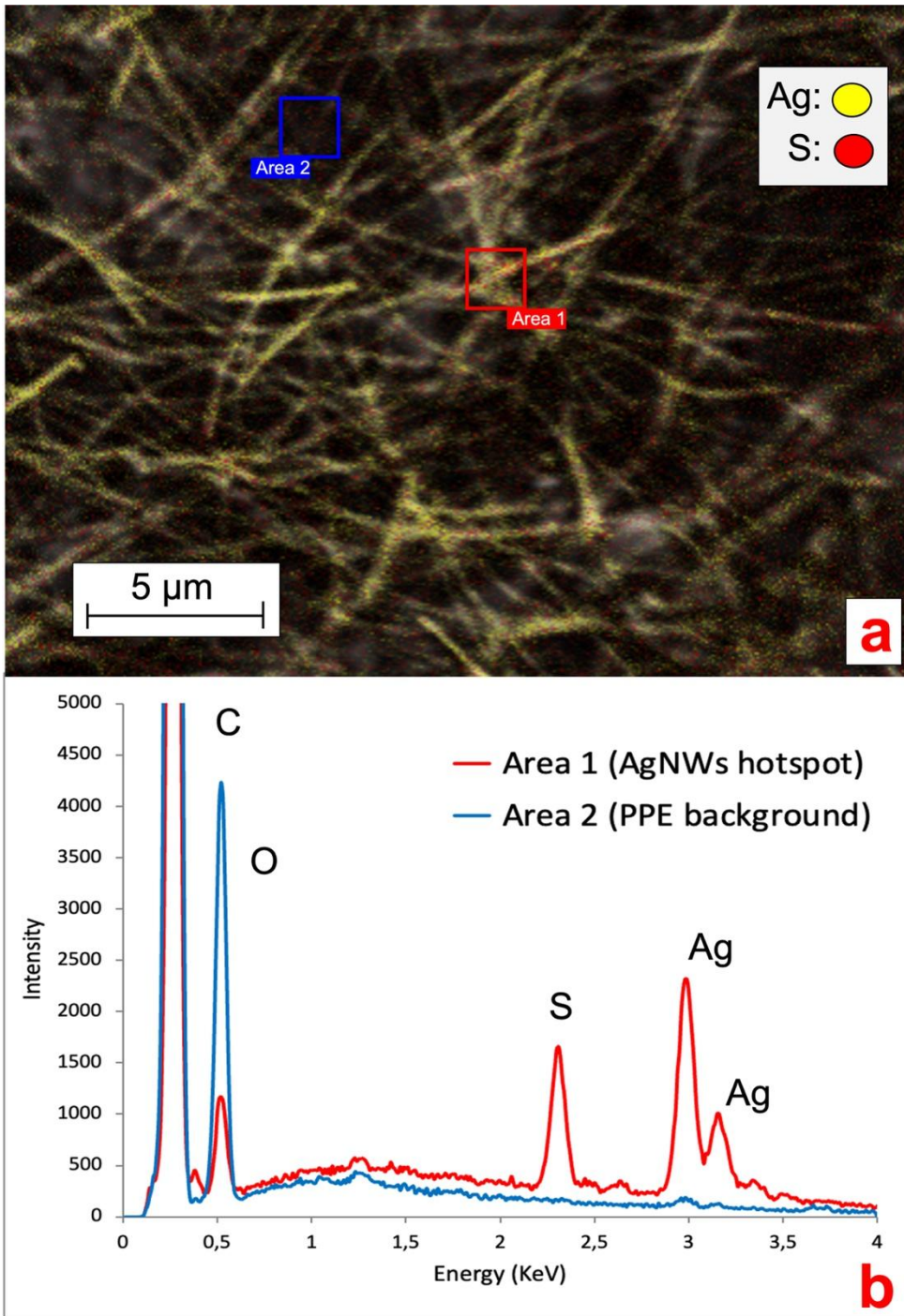
357 Of course, aging under abiotic conditions was a simplified exposure scenario compared to
358 mesocosms, as it did not account for all biodegradation mechanisms. On the other hand, it allowed
359 for an easier recovery of aged AgNWs-PPE fragments, which were analyzed to gather qualitative
360 information about the distribution, morphology and speciation of the AgNWs in the NEP during
361 aging.

362 Before aging, the AgNWs were homogeneously distributed onto one side of the NEP (Fig. 1b) where
363 they formed entanglements displaying protruding nano-structures as well as portions merged within
364 the cellulose matrix. The analysis at higher magnification (Fig. 1c) revealed an irregular (non-
365 hexagonal) morphology of the AgNWs, as well as the presence of NaCl nano-crystals (approx. 10 nm
366 diameter), confirmed by EDX analysis. The latter could be due to the presence of endogenous Cl
367 species in the samples owing to the PVDC coating.

368 As shown in Fig. 4, after 21d of batch incubation, changes in both the NEP matrix and AgNWs
369 morphology and distribution were observed. It must be noted that because of the drying process
370 prior to SEM analysis, an alteration of the cellulose matrix and of the AgNWs could have occurred.
371 With regard to the ENMs, as shown in Fig. 4a the AgNWs could still be identified onto the aged NEPs
372 surface, but presented extensive breakages and changes in morphology. Furthermore, the AgNWs
373 displayed a lower surface density compared to non-aged NEPs, and were all bound to the cellulose
374 matrix, with no protruding nanostructures.

375 The AgNWs density and distribution at the aged surfaces were further investigated by analyzing
376 larger NEPs areas. The detection at low energy (focused on the surface) showed that in aged
377 samples, the AgNWs were not homogeneously distributed onto the cellulose surface (Fig. 4b). Large
378 areas appeared empty and clusters of nanostructures could only be identified in hotspots.
379 Interestingly, the analysis of the same regions at higher energy (both surface and bulk detection)
380 revealed the presence of ENMs incorporated into the cellulose matrix, with distribution similar to
381 that of the original samples (Fig. 4c). These findings suggest that aging of the AgNWs-PPE affected
382 only the AgNWs immediately at the NEP surface, thus directly exposed to the outer environment.
383 However, the majority of the ENMs partially or totally incorporated in the matrix, not directly
384 exposed to weathering, presented a near original state. Hence, our hypothesis is that most of the Ag
385 recovered in the cellulose after 21 d of incubation was in the form of ENM, with morphology and
386 distribution resembling those of the original non-aged NEP. In general, these results are in
387 accordance with a recent study on AgNWs-PPE recycling, in which most of the ENMs were retained
388 in the matrix pulp due to embedding by cellulose nanofibrils(14).

389



390
 391
 392
 393
 394
 395
 396
 397

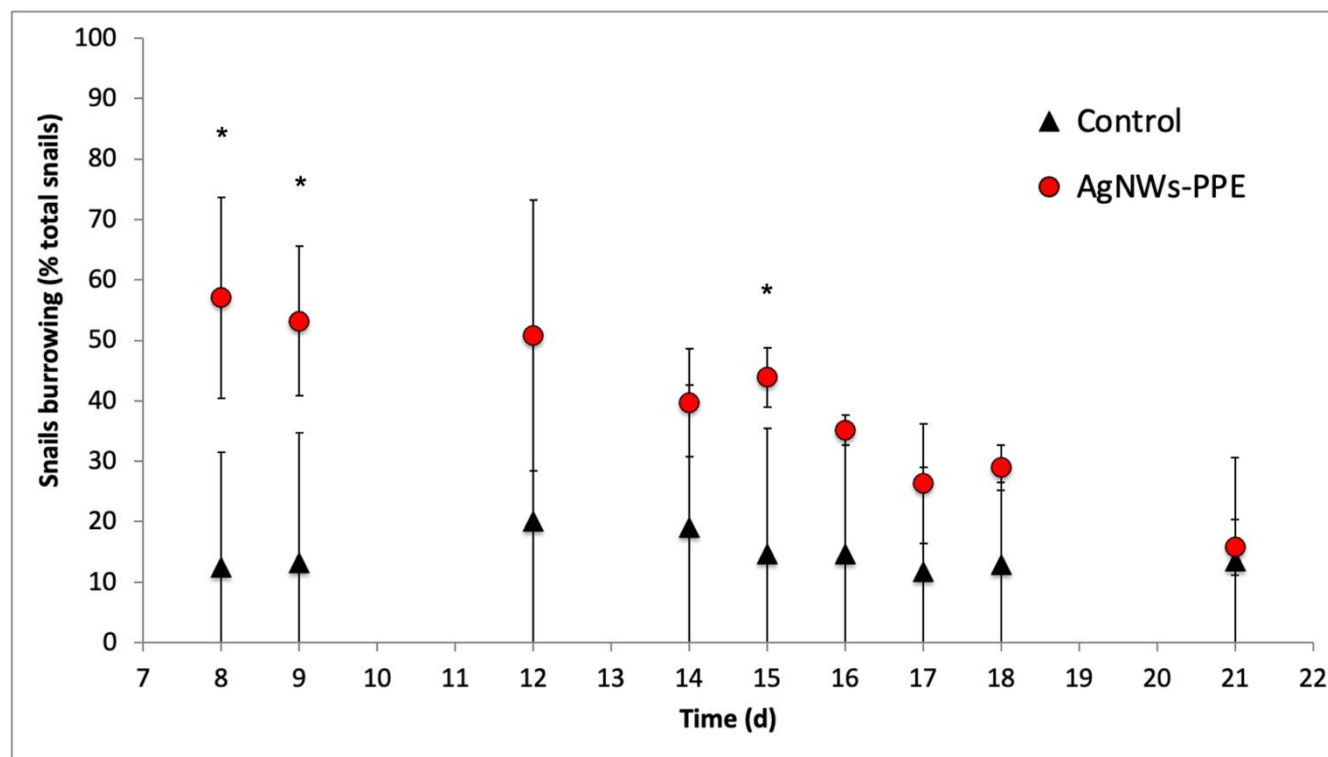
Fig. 5. a) SEM-EDX mapping at the surface of an aged AgNWs-PPE fragment from batch incubation. Silver and sulfur are represented in yellow and red colors, respectively. b) EDX spectra of two different locations in the map, namely a AgNWs hotspot (Area 1, red) and NEP background (Area 2, blue)

398 Ag-ENMs are known to undergo transformation processes in environmental media, with the
399 formation of novel Ag species (e.g. Ag sulfuration, AgCl complexes or precipitates)(10)(11)(19)(27).
400 Understanding the occurrence of such processes in NEPs is fundamental, since they can affect ENMs
401 stability, behavior and metal release in aqueous media(29)(30). Here, we collected EDX spectra of
402 the AgNWs at the AgNWs-PPE surface in order to investigate the potential changes in the chemical
403 composition and silver speciation. As shown in Fig. 5, in aged AgNWs-PPE we observed an important
404 sulfur signal in AgNWs hotspots, which was not recorded in the cellulose/PVDC NEPs background.
405 Further EDX mapping clarified the colocalization of Ag and S in AgNWs hotspots. In freshwater, Ag
406 sulfidation is a major transformation pathway for pristine Ag-ENMs. It has been extensively reported
407 in mesocosm studies(19)(27) and was linked to a reduced toxicity toward biota(31)(32). It must be
408 noted that sulfidized Ag-ENMs are often less soluble than their pristine counterparts, though Ag⁺ ion
409 solid diffusion may be high in the Ag₂S surface layer(33), and their formation in the PPE samples may
410 have enhanced their persistence in the nanoproduct.
411 The results obtained in the abiotic batch experiment presented here suggest that similar sulfidation
412 processes could also occur when the Ag-ENMs are incorporated in a NEPs, such as paper-based PPE.
413 However, future works will need to further characterize these processes in biotic experimental
414 conditions and in the natural environment.

415
416
417
418

3.3 Ecosystem effects induced by AgNW-based PPE

419



420 Figure 6. Percentage of benthic organisms *A. leucostoma* displaying a burrowing trait following
421 exposure to fragmented AgNMs-PPE (red circles) versus controls (black triangles). * highlights the
422 differences in mean \pm standard deviation (n=3) between the two treatments.

423

424 The environmental risk posed by a contaminant depends on its toxicity (hazard), speciation and
425 concentration (exposure) toward target ecological niches.

426 In the water column of the mesocosms exposed to AgNMs-PPE, the chronic contamination did not
427 induce significant effects on most biotic and abiotic parameters. Briefly, no significant changes were
428 observed in pH, redox potential and conductivity following AgNMs-PPE addition. The water TOC was
429 not significantly different, over the course of the incubation, between controls (1.71 ± 0.16 mg.L⁻¹ in
430 average) and contaminated mesocosms (1.75 ± 0.25 mg.L⁻¹ on average). The same was valid for
431 chlorophyll and suspended particle amounts as well as planktonic organism (*Daphnia* sp.) and
432 bacteria populations (Supplementary Information, S2). In general, the low impact on water
433 parameters can be attributed to the Ag speciation and the low Ag water concentration in the
434 mesocosms (Fig. 2b and Fig. 5, respectively).

435 On the other hand, the Ag accumulation in sediments implied a high exposure of the benthic
436 compartment, which was evaluated by monitoring the Ag bioaccumulation and burrowing behavior
437 of the aquatic snail *A. leucostoma*. Herein, Ag concentrations in *A. leucostoma* increased up to $43.4 \pm$
438 15.1 mg.kg⁻¹ (dw) at 14d and stabilized at 33.7 ± 8.2 mg.kg⁻¹ at 21d (Fig. 2c) following AgNMs-PPE
439 treatments. Interestingly, up to $96 \pm 5\%$ of the Ag was not leached from the snails after acidic wash
440 of the external bodies, suggesting that the Ag was ingested by the snail and not adsorbed onto the
441 shell surface. The stabilization of the Ag concentration taken up by the organism between day 14 and
442 21 could be due to the combination of both ingestion and depuration processes that are well known
443 in mollusks(23)(34). Such metals uptake/ingestion in benthic organisms has already been reported
444 after contamination with several pristine ENMs such as Ce-ENMs(26), Cu-ENMs(24) and Ag-
445 ENMs(23). In the case of NEPs, the Ag bioaccumulation in mud snails exposed in freshwater
446 mesocosms was attributed to a trophic transfer route from Ag-enriched biofilm(23). During the
447 present mesocosm experiment, we observed the direct feeding of snails on the AgNMs-PPE
448 fragments accumulated at the sediment/water interface and we hypothesize that the majority of Ag
449 bioaccumulation in snails was due to a direct uptake of AgNMs-PPE. This may have been enhanced
450 by both the cellulose in the NEP matrix, representing a potential food source for the organisms, and
451 the size of fragmented AgNMs-PPE directly bioavailable for the snails. It is noteworthy that the
452 concentrations in the snails observed in this study (~ 40 mg[Ag].Kg⁻¹ at 21d) were relatively high in
453 consideration of the low dose of total Ag introduced in the mesocosms (~ 50 ug [Ag].L⁻¹ at 21d). For
454 instance, similar levels (~ 100 mg [Ag].kg⁻¹) were observed in ecotoxicity tests with aquatic snails (*B.*
455 *glabrata*) exposed to Ag-ENMs at water concentrations up to 50 times higher(34).

456 Remarkably, despite significant Ag uptake no enhanced mortality of *A. leucostoma* adults was
457 observed during the experiment, suggesting no acute toxicity of the Ag from aged AgNMs-PPE for
458 the snails. However, the Ag species taken up did not necessarily enter the animal's systemic

459 circulation, and a low toxicity could be also related to sulfidation of the AgNWs at the surface of the
460 aged AgNWs-PPE (Figure 5), which is known to reduce noxious effects to aquatic biota(18)(31). In
461 addition, no significant effect was observed on benthic bacteria population density (Supplementary
462 information, S3). However, aquatic organisms can respond to stress with a combination of
463 physiological adaptation and behavior responses, which are known to occur after heavy metal
464 contamination(35), but are less studied in the case of ENMs and NEP(36). In freshwater snails, such
465 traits are observed as a response to drought and predation but also result as a consequence of
466 contamination(37). In the present study, we noticed an increased burrowing of the *A. leucostoma*
467 after one week of chronic contamination and monitored it until the end of the experiment. As shown
468 in Fig. 6, in mesocosms treated with AgNWs-PPE, the snail burrowing activity was observed in up to
469 $50\pm 7\%$ of the snails, on average, during the second week of experiment and $30\pm 10\%$ of the snails,
470 on average, during the third week. This was significantly higher than controls at d8, d9 and d15. Similar
471 stress responses, in mesocosms contaminated with ENMs, were reported by Buffet et al.,(36)(38)
472 who showed behavioral impairment (burrowing kinetic, feeding rate) of bivalve exposed to Cu- and
473 Ag-ENMs in seawater ecosystems.

474 It is worth comparing these biological effects with those observed in the mesocosm contaminated
475 with pristine AgNWs, which will be discussed in detail in a future study. Here, at d21 the sediments
476 were also the main sink for Ag, accumulating $92\pm 5\%$ of the total dose injected. Furthermore, the Ag
477 concentrations in snails were comparable to those observed in NEP treatments (33 ± 8 mg [Ag].kg⁻¹
478 for AgNWs-PPE and 69 ± 4 mg [Ag].kg⁻¹ for pristine AgNWs), despite the 10-fold higher total Ag
479 introduced in the mesocosms. However, in the pristine AgNWs treatment, no significant burrowing
480 alteration was observed in comparison to controls. These interesting results suggest that the altered
481 behavior following AgNWs-PPE treatments was not due to the absolute amount of Ag uptake.
482 Rather, it could be induced by a different physical-chemical state and speciation of the AgNWs in the
483 ingested AgNWs-PPE fragment compared to pristine ENMs, or due to a direct positive effect of the
484 PPE matrix uptake on the mollusc metabolism and behavior. Future studies will need to explore the
485 role of the cellulose matrix in the biodistribution and biotransformation of ENMs in aquatic
486 ecosystems more deeply, e.g. by including matrix-only treatments. A better understanding of
487 AgNWs-PPE effects on biota will also require the combination of behavioral traits observations, such
488 as burrowing, with other biological response analysis (e.g. biochemical markers analysis).

489

490

491 5. Environmental implications of paper-based NEPs

492

493 ENMs are being produced and applied in a wide range of NEPs(15), where they are incorporated into
494 a variety of liquid or solid formulations(39)(40)(41). Several studies recognize that the ENMs
495 integration in such matrices determines the properties of the materials that may be released
496 throughout the life cycle(42). Hence, the matrices can affect the behavior, fate and impact of ENMs
497 when compared to pristine nanoparticles, e.g. with regard to their partitioning in the ecosystem, the

498 metal release rates and speciation, and ecotoxicity effects(12)(43). Here, we investigated the fate
499 and effects of AgNWs incorporated into a cellulose/PVDC matrix for the construction of novel
500 AgNWs-PPE nanotechnologies.

501 In this study, the NEP matrix drove the fate of the incorporated ENMs, influencing their
502 environmental behavior and interaction with biota. In general, the PPE exposure potential (defined
503 as the potential to release ENMs and metals(7)) appeared to be low, and pond ecosystems
504 contaminated with AgNWs-PPE were exposed to ENMs-matrix complexes rather than free ENMs
505 and metals. Considering an environmental fate and risk perspective, we observed that the PPE
506 accumulated in the pond sediments, resulting in a fast removal of the Ag from the water column, but
507 also an enhanced exposure of the benthic compartment. A lower distribution in water does not
508 necessarily translate to a diminished environmental risk, but to a change in the magnitude to which
509 target ecological niches will be exposed. Indeed, a higher accumulation of the paper-based NEPs in
510 sediments may imply a higher ENMs exposure and bioavailability for benthic organisms, such as the
511 aquatic snails in the present study. Here, no acute toxicity was observed toward the snails, at
512 concentrations higher than those expected in real ecosystems(44). However, paper-based NEPs may
513 represent a food source for aquatic organisms, resulting in an enhanced bioaccumulation and
514 behavioral changes, which must be monitored for a proper assessment of NEPs impact and should be
515 explored more thoroughly by future studies.

516 We also observed that paper-based NEPs represent a very peculiar material, whose behavior could
517 be hard to predict compared to other matrices such as plastic or cement nano-composites(12). In
518 particular, the fragmented AgNWs-PPE is in principle a (bio)degradable product, but formed flocs
519 that accumulated at the sediment surface in the static mesocosm conditions. Due to the ease of
520 resuspension of such flocs, an enhanced transport may be expected in dynamic lotic environments,
521 such as rivers and flowing water. Future studies will need to address these questions, and to further
522 investigate the state at which paper-based NEPs enter and are transformed in the environment, as
523 well as their transport and removal from aquatic systems.

524 Accordingly, when grouping NEP fate and impact based on the matrix material, paper-based NEPs
525 may constitute a category of their own. This is also supported by recent studies testing food contact
526 release of nano-forms from packaging NEPs, which highlighted a different behavior of paper-based
527 NEPs compared to other materials such as polymeric matrices(45). The data and information
528 reported in this study will be useful for tracking and predicting the fate of ENMs embedded in similar
529 matrices.

530

531

532

533

534 Acknowledgement

535

536 This work was supported by the Excellence Initiative of Aix-Marseille University - A*MIDEX, a French
537 "Investissements d'Avenir" program, through its associated Labex SERENADE project. This work is
538 also a contribution to the OSU-Institut Pythéas. The authors acknowledge the CNRS funding for the
539 IRP iNOVE.

540

541

542 References

543

544

- 545 1. Rose J, Auffan M, de Garidel-Thoron C, Artous S, Auplat C, Brochard G, et al. The SERENADE
546 project; a step forward in the safe by design process of nanomaterials: The benefits of a diverse
547 and interdisciplinary approach. *Nano Today*. 2021 Apr;37:101065.
- 548 2. Liao X, Zhang Z, Liao Q, Liang Q, Ou Y, Xu M, et al. Flexible and printable paper-based strain
549 sensors for wearable and large-area green electronics. *Nanoscale*. 2016;8(26):13025–32.
- 550 3. Mitrano DM, Motellier S, Clavaguera S, Nowack B. Review of nanomaterial aging and
551 transformations through the life cycle of nano-enhanced products. *Environment International*.
552 2015 Apr;77:132–47.
- 553 4. Li W, Yang S, Shamim A. Screen printing of silver nanowires: balancing conductivity with
554 transparency while maintaining flexibility and stretchability. *npj Flex Electron*. 2019 Dec;3(1):13.
- 555 5. Li W, Yarali E, Bakytbekov A, Anthopoulos TD, Shamim A. Highly transparent and conductive
556 electrodes enabled by scalable printing-and-sintering of silver nanowires. *Nanotechnology*. 2020
557 Sep 25;31(39):395201.
- 558 6. Liu J, Yang C, Wu H, Lin Z, Zhang Z, Wang R, et al. Future paper based printed circuit boards for
559 green electronics: fabrication and life cycle assessment. *Energy Environ Sci*. 2014;7(11):3674–82.
- 560 7. Moeta PJ, Wesley-Smith J, Maity A, Thwala M. Nano-enabled products in South Africa and the
561 assessment of environmental exposure potential for engineered nanomaterials. *SN Appl Sci*.
562 2019 Jun;1(6):577.
- 563 8. Benn TM, Westerhoff P. Nanoparticle Silver Released into Water from Commercially Available
564 Sock Fabrics. *Environ Sci Technol*. 2008 Jun 1;42(11):4133–9.
- 565 9. Geranio L, Heuberger M, Nowack B. The Behavior of Silver Nanotextiles during Washing. *Environ*
566 *Sci Technol*. 2009 Nov 1;43(21):8113–8.
- 567 10. Lorenz C, Windler L, von Goetz N, Lehmann RP, Schuppler M, Hungerbühler K, et al.
568 Characterization of silver release from commercially available functional (nano)textiles.
569 *Chemosphere*. 2012 Oct;89(7):817–24.

- 570 11. Lombi E, Donner E, Scheckel KG, Sekine R, Lorenz C, Goetz NV, et al. Silver speciation and
571 release in commercial antimicrobial textiles as influenced by washing. *Chemosphere*. 2014
572 Sep;111:352–8.
- 573 12. Amorim MJB, Lin S, Schlich K, Navas JM, Brunelli A, Neubauer N, et al. Environmental Impacts by
574 Fragments Released from Nanoenabled Products: A Multiassay, Multimaterial Exploration by the
575 SUN Approach. *Environ Sci Technol*. 2018 Feb 6;52(3):1514–24.
- 576 13. Pourzahedi L, Vance M, Eckelman MJ. Life Cycle Assessment and Release Studies for 15
577 Nanosilver-Enabled Consumer Products: Investigating Hotspots and Patterns of Contribution.
578 *Environ Sci Technol*. 2017 Jun 20;51(12):7148–58.
- 579 14. Zareeipolgardani B, Piednoir A, Joyard-Pitiot B, Depres G, Charlet L, Colombani J. Multiscale
580 investigation of the fate of silver during printed paper electronics recycling. *Composite*
581 *Interfaces*. 2022 Sep 30;1–14.
- 582 15. Nowack B, Boldrin A, Caballero A, Hansen SF, Gottschalk F, Heggelund L, et al. Meeting the
583 Needs for Released Nanomaterials Required for Further Testing—The SUN Approach. *Environ*
584 *Sci Technol*. 2016 Mar 15;50(6):2747–53.
- 585 16. Masion, Auffan, Rose. Monitoring the Environmental Aging of Nanomaterials: An Opportunity
586 for Mesocosm Testing? *Materials*. 2019 Jul 31;12(15):2447.
- 587 17. Auffan M, Masion A, Mouneyrac C, de Garidel-Thoron C, Hendren CO, Thiery A, et al.
588 Contribution of mesocosm testing to a single-step and exposure-driven environmental risk
589 assessment of engineered nanomaterials. *NanoImpact*. 2019 Jan;13:66–9.
- 590 18. Carboni A, Slomberg DL, Nassar M, Santaella C, Masion A, Rose J, et al. Aquatic Mesocosm
591 Strategies for the Environmental Fate and Risk Assessment of Engineered Nanomaterials.
592 *Environ Sci Technol*. 2021 Dec 21;55(24):16270–82.
- 593 19. Lowry GV, Espinasse BP, Badireddy AR, Richardson CJ, Reinsch BC, Bryant LD, et al. Long-Term
594 Transformation and Fate of Manufactured Ag Nanoparticles in a Simulated Large Scale
595 Freshwater Emergent Wetland. *Environ Sci Technol*. 2012 Jul 3;46(13):7027–36.
- 596 20. Auffan M, Tella M, Santaella C, Brousset L, Paillès C, Barakat M, et al. An adaptable mesocosm
597 platform for performing integrated assessments of nanomaterial risk in complex environmental
598 systems. *Sci Rep*. 2014;4(1):5608.
- 599 21. Colman BP, Baker LF, King RS, Matson CW, Unrine JM, Marinakos SM, et al. Dosing, Not the
600 Dose: Comparing Chronic and Pulsed Silver Nanoparticle Exposures. *Environ Sci Technol*. 2018
601 Sep 4;52(17):10048–56.
- 602 22. Avellan A, Simonin M, McGivney E, Bossa N, Spielman-Sun E, Rocca JD, et al. Gold nanoparticle
603 biodissolution by a freshwater macrophyte and its associated microbiome. *Nature Nanotech*.
604 2018 Nov;13(11):1072–7.

- 605 23. Cleveland D, Long SE, Pennington PL, Cooper E, Fulton MH, Scott GI, et al. Pilot estuarine
606 mesocosm study on the environmental fate of Silver nanomaterials leached from consumer
607 products. *Science of The Total Environment*. 2012 Apr;421-422:267-72.
- 608 24. Auffan M, Liu W, Brousset L, Scifo L, Pariat A, Sanles M, et al. Environmental exposure of a
609 simulated pond ecosystem to a CuO nanoparticle-based wood stain throughout its life cycle.
610 *Environ Sci: Nano*. 2018;5(11):2579-89.
- 611 25. Amiard-Triquet C. Behavioral Disturbances: The Missing Link between Sub-Organismal and
612 Supra-Organismal Responses to Stress? Prospects Based on Aquatic Research. *Human and
613 Ecological Risk Assessment*. 2009;15(1):87-110.
- 614 26. Tella M, Auffan M, Brousset L, Issartel J, Kieffer I, Pailles C, et al. Transfer, Transformation, and
615 Impacts of Ceria Nanomaterials in Aquatic Mesocosms Simulating a Pond Ecosystem. *Environ Sci
616 Technol*. 2014 Aug 19;48(16):9004-13.
- 617 27. Auffan M, Santaella C, Brousset L, Tella M, Morel E, Ortet P, et al. The shape and speciation of Ag
618 nanoparticles drive their impacts on organisms in a lotic ecosystem. *Environ Sci: Nano*.
619 2020;7(10):3167-77.
- 620 28. Furtado LM, Hoque ME, Mitrano DM, Ranville JF, Cheever B, Frost PC, et al. The persistence and
621 transformation of silver nanoparticles in littoral lake mesocosms monitored using various
622 analytical techniques. *Environ Chem*. 2014;11(4):419.
- 623 29. Lowry GV, Gregory KB, Apte SC, Lead JR. Transformations of Nanomaterials in the Environment.
624 *Environ Sci Technol*. 2012 Jul 3;46(13):6893-9.
- 625 30. Lead JR, Batley GE, Alvarez PJJ, Croteau MN, Handy RD, McLaughlin MJ, et al. Nanomaterials in
626 the environment: Behavior, fate, bioavailability, and effects-An updated review: Nanomaterials
627 in the environment. *Environ Toxicol Chem*. 2018 Aug;37(8):2029-63.
- 628 31. Yuan L, Richardson CJ, Ho M, Willis CW, Colman BP, Wiesner MR. Stress Responses of Aquatic
629 Plants to Silver Nanoparticles. *Environ Sci Technol*. 2018 Mar 6;52(5):2558-65.
- 630 32. Lehmann SG, Toybou D, Pradas del Real AE, Arndt D, Tagmount A, Viau M, et al. Crumpling of
631 silver nanowires by endolysosomes strongly reduces toxicity. *Proc Natl Acad Sci USA*. 2019 Jul
632 23;116(30):14893-8.
- 633 33. Simonnin P, Sassi M, Gilbert B, Charlet L, Rosso KM. Phase Transition and Liquid-like Superionic
634 Conduction in Ag₂S. *J Phys Chem C*. 2020 May 7;124(18):10150-8.
- 635 34. Oliveira-Filho E, Muniz D, Carvalho E, Cáceres-Velez P, Fascineli M, Azevedo R, et al. Effects of
636 AgNPs on the Snail *Biomphalaria glabrata*: Survival, Reproduction and Silver Accumulation.
637 *Toxics*. 2019 Mar 1;7(1):12.
- 638 35. McInnes JR, Thurberg FP. Effects of metals on the behaviour and oxygen consumption of the
639 mud snail. *Mar Pollut Bull*. 1973;4:185-7.

- 640 36. Buffet PE, Tankoua OF, Pan JF, Berhanu D, Herrenknecht C, Poirier L, et al. Behavioural and
641 biochemical responses of two marine invertebrates *Scrobicularia plana* and *Hediste diversicolor*
642 to copper oxide nanoparticles. *Chemosphere*. 2011 Jun;84(1):166–74.
- 643 37. Hazelton PD, Du B, Haddad SP, Fritts AK, Chambliss CK, Brooks BW, et al. Chronic fluoxetine
644 exposure alters movement and burrowing in adult freshwater mussels. *Aquatic Toxicology*. 2014
645 Jun;151:27–35.
- 646 38. Buffet PE, Pan JF, Poirier L, Amiard-Triquet C, Amiard JC, Gaudin P, et al. Biochemical and
647 behavioural responses of the endobenthic bivalve *Scrobicularia plana* to silver nanoparticles in
648 seawater and microalgal food. *Ecotoxicology and Environmental Safety*. 2013 Mar;89:117–24.
- 649 39. Botta C, Labille J, Auffan M, Borschneck D, Miche H, Cabie M, et al. TiO₂-based nanoparticles
650 released in water from commercialized sunscreens in a life-cycle perspective: Structures and
651 quantities. *Environmental Pollution*. 2011 June;159(6):543–1550.
- 652 40. Bossa N, Chaurand, Perrine, Levard C, Borschneck D, Miche H, Vicente J, et al. Environmental
653 exposure to TiO₂ nanomaterials incorporated in building material. *Environ Pollut*.
654 2017;220:1160–70.
- 655 41. Scifo L, Chaurand P, Bossa N, Avellan A, Auffan M, Masion A, et al. Non-linear release dynamics
656 for a CeO₂ nanomaterial embedded in a protective wood stain, due to matrix photo-degradation.
657 *Environmental Pollution*. 2018 Oct;241:182–93.
- 658 42. Liu S, Xia T. Continued Efforts on Nanomaterial-Environmental Health and Safety Is Critical to
659 Maintain Sustainable Growth of Nanoindustry. *Small*. 2020;16(21).
- 660 43. Wohlleben W, Hellack B, Nickel C, Herrchen M, Hund-Rinke K, Kettler K, et al. The nanoGRAVUR
661 framework to group (nano)materials for their occupational, consumer, environmental risks based
662 on a harmonized set of material properties, applied to 34 case studies. *Nanoscale*.
663 2019;11(38):17637–54.
- 664 44. Giese B, Klaessig F, Park B, Kaegi R, Steinfeldt M, Wigger H, et al. Risks, Release and
665 Concentrations of Engineered Nanomaterial in the Environment. *Sci Rep*. 2018 Dec;8(1):1565.
- 666 45. Ruggiero E, Santizo KY, Persson M, Delpivo C, Wohlleben W. Food contact of paper and plastic
667 products containing SiO₂, Cu-Phthalocyanine, Fe₂O₃, CaCO₃: Ranking factors that control the
668 similarity of form and rate of release. *NanoImpact*. 2022 Jan;25:100372.

669
670
671
672
673
674

